

Shielding the Skull: Exploring the Influence of Facial Protection, Impact Location and Neck Stiffness on Hockey Helmet Safety During a Linear Impact

Leigh Jeffries^{*1}, Meilan Liu^{#2}, Paolo Sanzo^{*1}, Eryk Przysucha^{*1}, Carlos Zerpa^{*1}

¹School of Kinesiology, ²Department of Mechanical and Mechatronics Engineering, Lakehead University, ON, Canada

*Denotes student investigator, #Denotes established investigator

Abstract

International Journal of Exercise Science 18(7): 343-362, 2025.

<https://doi.org/10.70252/REVL1750> Originally designed to mitigate skull fractures and traumatic brain injuries in hockey players, hockey helmets have now become a critical focus for further research due to the rise in mild traumatic brain injuries. With the sport's evolution introducing stronger and faster players, new approaches that incorporate facial shielding in helmet technology and enhance athletes' neck strength are needed to reduce concussion risks. This study pursued two primary objectives. Firstly, it sought to determine if a hockey helmet's stiffness fluctuated at different contact locations during static compression with the inclusion of facial shielding. Secondly, it examined the influence of impact location, facial protection type, and neck stiffness on head injury risk during simulated dynamic impacts, gauged by the Gadd Severity Index (GSI). The findings revealed that helmet stiffness varied across locations, and a significant three-way interaction was observed between facial shielding, impact location, and neckform stiffness level concerning GSI measures at $p < 0.05$. Further analysis unveiled significant two-way interactions between impact location and facial shielding across neck strength levels at $p < 0.05$. These outcomes underscore the critical role of facial shielding, neck strength and impact location, in averting brain injuries in hockey. The results carry practical implications for helmet manufacturers, standards bodies, coaches, and players, urging a comprehensive approach to helmet design and player safety.

Keywords: Head impact locations, risk of head injury, concussions, headform, neckform

Introduction

Ice hockey is a dynamic and physically demanding sport that exposes players to a considerable risk of injury.¹ Head injuries, in the sport of ice hockey, can have severe repercussions on a player's health and quality of life.² Head injuries that frequently occur in hockey are concussions or mild traumatic brain injuries (mTBI). A concussion occurs when the head or torso experiences static or dynamic loading forces, temporarily affecting brain function³ and causing symptoms such as alterations in consciousness, amnesia, visual disturbances, concentration problems, headache, vertigo, and balance disturbances.⁴

In the last decade, concussion accounts for 14-30% of hockey-related head injuries with rates of 5.8-6.1 concussions for 100 games according to data collected from the National Hockey League (NHL) Players' Association.⁵ When a player is struck in the head, the kinematic response of the brain and neural damage upon the head impact depends on: a) the acceleration of the impact; b) the location of the impact on the head; c) the level of neck strength of the athlete; and d) the type of head protection.⁶

Understanding the type of impact acceleration that occurs to the head is crucial in assessing the potential risk of injury and concussion that may result from an impact. When the head experiences linear impact acceleration, it undergoes a forward or backward motion without any rotational movement.⁷ This type of impact acceleration can cause various injuries, including skull fractures, brain contusions, and diffuse axonal injury (DAI), especially if the head collides with an object.^{7,8}

Gurdjian⁹ proposed that a linear acceleration of 80-90 g (g is the gravitational acceleration; g = 9.81 m/s²) for greater than 4 ms (milliseconds) would result in a higher risk of concussion. Comparatively, Zhang et al⁸ suggested that a peak resultant linear acceleration of 66 g, 82 g, and 106 g at the centre of gravity of the head corresponds to a 25%, 50%, and 80% probability of sustaining a concussion, respectively. These thresholds were derived from typical impact durations of 10-16 ms.

The risk of head injury, and ultimately the risk of concussion, is measured based on the area under the linear acceleration-time curve to form the basis for a GSI index¹⁰ as shown in Equation 1. A weighting factor of 2.5 is applied to the acceleration value to discriminate between impacts with varying levels of risk.¹⁰

$$GSI = \int_{t_0}^{t_1} A^{2.5} dt \quad (1)$$

where:

A = instantaneous resultant acceleration of the headform

t₀, t₁ = time instants when impact begins and ends, respectively; t₁ - t₀ gives the impulse duration

dt = time increment

The location where a player typically sustains a head impact may have implications on the risk level of head injury due to the dynamic response of the human skull and brain tissue. Zhang et al¹¹ conducted studies revealing that lateral impacts to the head resulted in increased stress levels and greater chances of skull deformation. Hodgson et al¹² also conducted research to determine concussion tolerances for various impact sites and found that side locations resulted in longer periods of unconsciousness and higher linear impact accelerations. The researchers

concluded that the oval geometry and thinner bones in the side region of the head might lead to increased concussion tolerance and acceleration. Similarly, Walsh et al¹³ discovered differences in peak linear acceleration when impacting the head at different locations. However, in terms of ranking impact locations by levels of peak linear acceleration, the findings were not consistent. Hodgson et al¹² found that side impacts resulted in the largest peak linear acceleration, followed by the front and rear locations. Carlson,¹⁴ however, found that the front boss impact site was the most susceptible to the highest peak linear acceleration, followed by the front, side, rear, and rear boss locations. The front boss is the location on the helmet that aligns with the side of the forehead, above the temple, and slightly forward of the middle of the head when looking from the side. The rear boss location is the location on the helmet that aligns with the side of the back of the head, above and behind the ear, and slightly behind the middle of the head when viewed from the side as shown in Figure 2b.

Research suggests that neck stiffness and helmet integrity are crucial in minimizing the risk of concussion by reducing head acceleration and effectively managing impact forces.^{15, 16, 17} In addition to wearing a helmet, athletes can improve their ability to withstand impact forces and minimize the risk of head injury by conditioning their head, neck, and trunk muscles to work together.¹⁶ Untrained athletes, particularly those with weaker necks, may be more susceptible to injury from impact accelerations.¹⁶ These research studies, however, have only examined the response of human neck stiffness during simulated head collisions using a headform with a mechanical neck attached. Nonetheless, researchers believe that neck stiffness and helmet materials affect the linear acceleration transmitted to the head and brain during a collision.¹⁶ Therefore, it is important to consider the effect of neck stiffness in helmet testing.

In the sport of ice hockey, helmets are the primary form of head protection and are mandatory for players at all levels of play.¹⁸ Current helmets designed by the manufacturers have masses ranging 0.545-0.578 kg. The thickness of the front outer shell ranges 2.5-2.9 mm, while the foam thickness ranges 14.1-19.4 mm in vinyl nitrile (VN) helmets, and 15.6-23.6 mm in expanded polypropylene (EPP) helmets.¹⁹ It should be noted that most hockey helmet materials fall somewhere between a plastic and elastic response.¹⁰ A plastic response of a hockey helmet means that there is irreversible damage to the helmet on impact. This response is most pertinent to the outer shell of the helmet, which may not fully restore its shape after many impacts. Alternatively, the foam liner of the helmet exhibits an elastic response. Upon contact, it deforms and then regains its original shape.²⁰ Deformation and restoration of the shape of the helmet material increases the capability of the helmet to protect the head.

When the helmets are tested to be certified, they are tested to meet the current criteria set forth by standard organizations. For example, the National Operating Committee on Standards for Athletic Equipment (NOCSAE) tests the helmets at six different locations: the front, right side, right front boss, right rear boss, rear, and top.²¹ Each location is impacted at 3.46 m/s, 4.88 m/s, and 5.46 m/s, respectively. No impacts should produce a GSI greater than 1,200, while a 3.46 m/s impact should not see a GSI greater than 300.²² This method of assessment was seen to be more suited to research, development, and the potential prediction of serious injury onset.²²

Helmets also include facial shields. The face shields are made of impact-resistant plastic such as polycarbonate or metal and are mounted to the brim on the front of the helmet in the mid-sagittal plane to reduce the risk of injury to the athlete's face due to impacts from a hockey puck or stick.^{18, 23} Facial protection has been found to reduce the incidence of ocular, facial, and dental injuries by 70%.^{24, 25}

Currently, there is a lack of evidence from clinical studies to indicate a connection between the use of face shields and a reduced risk of concussion.²⁶ There is scientific evidence, however, that supports the use of full facial shields in ice hockey to protect athletes from more severe concussions, as measured by time lost from competition.²⁶ Benson et al²⁶ emphasized the need for future research to focus on sport-specific, analytical studies with sufficient power to determine the true relative risk of concussion associated with specific types of protective equipment. Additionally, there is a lack of information regarding the combined effect of factors such as impact location, neck strength, and facial shields on the risk of head injuries, and more specifically the risk of concussions, during linear impact collisions.

Therefore, the first purpose of this study was to investigate the effect of facial shielding and helmet location on measures of helmet stiffness during static testing. Stiffness is defined as the amount of force needed to cause a certain amount of deformation of the material under compression.²⁷ The question guiding this purpose was: How do different facial shielding configurations affect the structural integrity and material behavior of helmets under static compression tests at different helmet locations? The researchers hypothesized that full facial metal shields would increase helmet stiffness under static compression, with effects varying by helmet location due to load distribution and structural reinforcement.

The second purpose was to examine the effect of impact location, type of facial protection, and neck stiffness level on GSI during dynamic simulated horizontal impacts. The research question guiding this purpose was: Does the location of impact, type of facial protection, and level of neck stiffness significantly affect GSI values during dynamic simulated horizontal impacts? The researchers hypothesized that the lowest GSI values would occur during dynamic horizontal impacts with full facial protection and high neck stiffness, particularly at the side impact location, due to the force distribution capability of the helmet at this location.

Methods

Participants

This study did not involve human participants; therefore, ethical approval was not required. This research, however, was carried out fully in accordance with the ethical standards of the International Journal of Exercise Science.²⁸ The study focused on simulating dynamic head collisions of hockey players, using a methodology similar to that of Zerpa et al²⁹ and Pennock et al.¹⁵ A power of analysis was conducted for a three-way mixed factorial analysis of variance (ANOVA) to determine the number of trial cases needed to simulate the hockey players' dynamic head collisions for a combination of 3 independent neck strength levels (low, medium and high), 3 repeated measures of face shield conditions (no facial shield, metal shield and

polycarbonate shield), and 5 repeated measures of helmet locations (front, front boss, side, rear and rear boss) as defined by NOCSAE testing standards.²¹ A sample of 15 cases was generated using the G-Power software to simulate the hockey players' head collisions for a power of rejection of 80%, alpha level of .05, and effect size-eta-square of .14.

Protocol

Instruments.

Five medium-sized identical hockey helmets with VN attenuation liners were used for the static and dynamic impact testing. The helmets were medium-sized (54-59 cm head circumference) and contained a dual-density VN liner along with a lightweight ventilated outer shell. The helmets were certified by Canadian Standards Association (CSA), Hockey Equipment Certification Council (HECC), and International Organization for Standards (ISO). The researchers tested the durability of the helmet using a similar approach as Carlson¹⁴ and determined that a helmet would receive 54 impacts in one location before being replaced to maintain the integrity of the data.

An Instron® device was used to study the static material properties of the helmet with and without facial shields by compressing the front, rear, and side locations as shown in Figure 1. The front boss and rear boss locations were not examined due to the limitations of the Instron® device to accommodate these sites. The hardware of the Instron® 1000 was connected to a data acquisition board and the LabVIEW software from National Instruments (NI®) to measure the compressive forces and deflection of the helmet material.

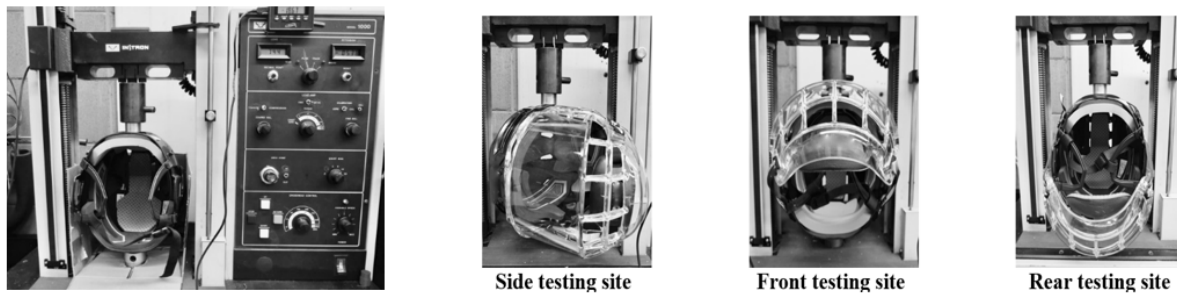


Figure 1. Instron® 1000 mechanical device and testing locations.

A pneumatic linear impactor was used to simulate the dynamic head collisions. The impactor consisted of several components including a main frame, an impacting rod with a mass of 13.1 kg, a compressed-air tank, a headform-neckform assembly, and a linear bearing table as shown in Figure 2. By releasing pressure from the 3-gallon compressed-air tank, the impact rod was propelled from the upper main frame at speeds ranging 2.01-5.13 m/s. The researchers used a Sintered Specialties Inc (SSI®) digital pressure gauge with an accuracy of $\pm 1\%$ full scale to control the released pressure. After each impact, the linear bearing table moved backward 0.49 m on rollers. The tip of the impact rod consisted of a cylindrical nylon cap with a diameter of 7.4 cm and a thickness of 2.7 cm.

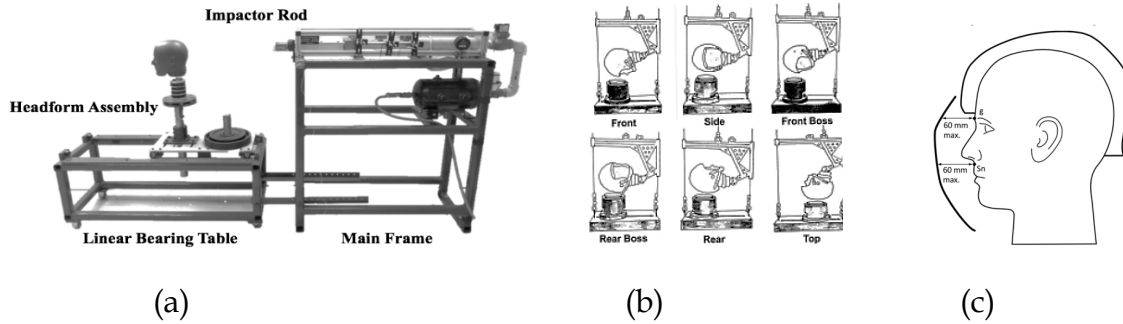


Figure 2. a) Pneumatic linear impactor, b) Impact locations as defined by NOCSAE standards (NOCSAE, 2020). Adapted from “Standard test method and equipment used in evaluating the performance characteristics of headgear/equipment”, National Operating Committee on Standards for Athletic Equipment, 2020, and c) Maximum allowed distance from headform to facial protector. Retrieved from “Face protectors for use in ice hockey,” (Z262.2-15 R2019), Toronto, Canada: CSA. Copyright 2015 by Canadian Standards Association.

A 4.90 kg NOCSAE headform as shown in Figure 2, instrumented with high-frequency tri-axial linear accelerometers, was used to simulate the dynamic response of the impact trials, similar to previous research work.^{14, 19, 29} The accelerometers were interfaced to a PCB model 482A04 integrated circuit piezoelectric sensor (ICP) amplifier/power supply unit. The analog output signals from the accelerometers were amplified and converted to digital signals via an analog to digital converter from AD Instruments® PowerLab26T. The headform was mounted on a mechanical neck. The mechanical neck consisted of four neoprene rubber discs fitted between circular steel discs with end plates at the top and bottom. To keep the components firmly pressed together, a galvanized stainless steel wire cable ran longitudinally through the centre of the rubber and steel discs including the end plates.¹⁴ To prevent movement of the steel and rubber discs, the rubber discs protrude from the metal discs slightly, allowing for the metal and rubber discs to be compressed tightly together. A top plate and base end plate held the components of the neck together by tightening a nut connected to the galvanized steel wire cable at the base of the neck assembly. This mechanism allowed the researchers to adjust the stiffness of the mechanical neck and the degree to which the neck rotated and flexed during impacts.¹⁵

A metal facial shield and a high-impact polycarbonate full-face shield were tested separately for this study. The facial shields were connected to the brim of the helmet in the mid-sagittal plane. Two screws held the cage in place and acted as the pivot point to allow the helmet to be taken on and off the headform.

Procedure.

For the static testing, stiffness measures were conducted at the front, rear, and side locations of the helmet without the face shield, with the metal facial shield, and with the high-impact polycarbonate facial shield, respectively, using the Instron® 1000 device, as depicted in Figure 1. The Instron® device utilized a 31.75-mm-diameter cylinder to apply force and compress the material at the speed of 25 mm per minute. Force measures in Newtons and material compression in mm were collected using a built-in Labview® script interfaced to the Instron® hardware. The data was exported to a Microsoft® Excel spreadsheet. A linear regression

function was used to represent the relationship between the force and compression (or deformation hereinafter) of the helmet material.

For the dynamic testing, the researchers properly fitted the helmet to the headform adhering to the manufacturer's instructions, ensuring that the foam liner contacted the headform, and consistently measuring 50 mm from the brim of the helmet to the bridge of the nose before each impact. The distance from the headform to the facial shield at the level of the brow and philtrum were also standardized. The standards for testing in Canada state that these distances should not exceed 60 mm as shown in Figure 2. Similarly, the facial shields were also attached to the helmets according to the manufacturer's instructions and CSA standards¹¹ when facial shields were tested with the helmet. The chin cap firmly affixed to the chin of the surrogate headform. Individual players, however, may wear their masks differently based on personal comfort, facial structure, or preference, which can result in variations in the fit of the chin cap. For this study, standardization was essential to obtain consistent and comparable data. Therefore, the helmet and its components were affixed to the headform according to manufacturer's guidelines, which might not account for all individual variations in fit.

The helmet was impacted one single time for each combination of neckform stiffness level, impact location and facial shielding condition across 18 different speeds ranging 2.01-5.13 m/s.¹⁴ This approach was used to simulate 18 hockey players being hit at different impact velocities, resulting in a total of 810 impacts for 45 different impact conditions. The neck stiffness was, 0.95 N·m (8.4 in·lb) for a low level, 1.36 N·m (12 in·lb) for a medium level, and 1.76 N·m (15.6 in·lb) for a high level, respectively.¹⁴ As previously stated, the neck stiffness levels were obtained by tightening a nut connected to the galvanized cable at the base of the mechanical neck assembly. The researchers switched helmets every 54 impacts per location to protect the integrity of the data due to wear and tear.¹⁴ The data was collected at a sampling frequency of 20,000 Hertz.

Statistical Analysis

The three-way mixed factorial ANOVA was used to examine the interaction effect between neck stiffness level, impact location, and facial shielding condition on GSI measures. To help explain the interactions, two-way mixed factorial ANOVAs were implemented to examine the interactions between facial shielding condition and helmet impact location on GSI measures for each neck strength level, respectively. The effect sizes for the ANOVA interactions and main effects were reported using eta squared (η^2) and interpreted according to Cohen's guidelines where 0.01 indicated a small effect, 0.06 indicated a medium effect, and 0.14 indicated a large effect. Post hoc analyses using one-way ANOVAs and Bonferroni's tests were conducted for mean comparisons.

Results

Helmet Stiffness Testing

The results in Figure 3 depict the helmet stiffness measures at the front, rear, and side locations, at each of the three facial shielding conditions: no facial shield (NFS), metal facial shield (MFS),

and high impact polycarbonate facial shield (PFS). The stiffness measures of the different conditions were compared using ratios of the slopes of the different linear regression lines. The nine unique stiffness testing conditions allow for a total of 72 comparisons to be made. The comparisons that seemed most relevant were those that revealed how the facial shield condition changed the stiffness properties of the helmet across locations of the helmet.

At the front location, the ratio for the stiffness of the MFS and NFS conditions (ratio = $16.93/6.79$) indicated that the helmet with MFS required 2.49 times more force to acquire the same deformation as when the helmet had NFS. Similarly, the ratio calculations revealed that the PFS requires 1.77 times more force to deform the helmet when compared to NFS (ratio = $12.04/6.79$). Finally, the ratio comparing the helmets with metal and polycarbonate shielding (ratio = $16.93/12.04$) indicated that the MFS condition required 1.41 times more force to produce an identical deformation as the helmet with the PFS.

When the helmet was tested at the rear and side locations, the facial shields also increased the amount of force required to produce identical deformations. At the rear location, force requirements to deform the helmet were increased to 2.54 times by the MFS (ratio = $19.90/7.83$) and 1.53 times by the PFS (ratio = $12.04/7.83$). At the side location, the force requirements for identical helmet deformation were 2.49 times more in a helmet with the MFS (ratio = $9.71/3.90$) and 2.48 more for the helmet with the PFS (ratio = $9.59/3.90$), respectively. Finally, the MFS condition increased the force requirements for equal deformation by 1.57 and 1.01 more times at the rear and side locations, respectively, compared to the PFS (ratio = $19.90/12.69$; ratio = $9.71/9.59$).

When comparing the slopes of the three compression locations on the helmet with respect to the three facial shielding conditions, it was determined that the rear location required the most force for deformation, followed by the front and side locations. To quantify the magnitude of the difference, ratios were once again used. On the helmet with NFS, the rear was 2.01, and 1.15 times as stiff as the side and front location, respectively (ratio = $7.83/3.90$; ratio = $7.83/6.79$). The front was also 1.74 times as stiff as the side (ratio = $6.79/3.90$). Similarly, the helmet with the MFS, made the rear location 2.05 and 1.18 times as stiff as the side and front locations, respectively (ratio = $19.90/9.71$; ratio = $19.90/16.93$). The front location, however, was 1.74 times as stiff as the side (ratio = $16.93/9.71$). Finally, the helmet with the PFS required 1.32 and 1.05 times the force to deform the rear location as compared to the side and the front locations (ratio = $12.69/9.59$; ratio = $12.69/12.04$). The PFS condition also caused the front to be 1.26 times as stiff as the side location (ratio = $12.04/9.59$).

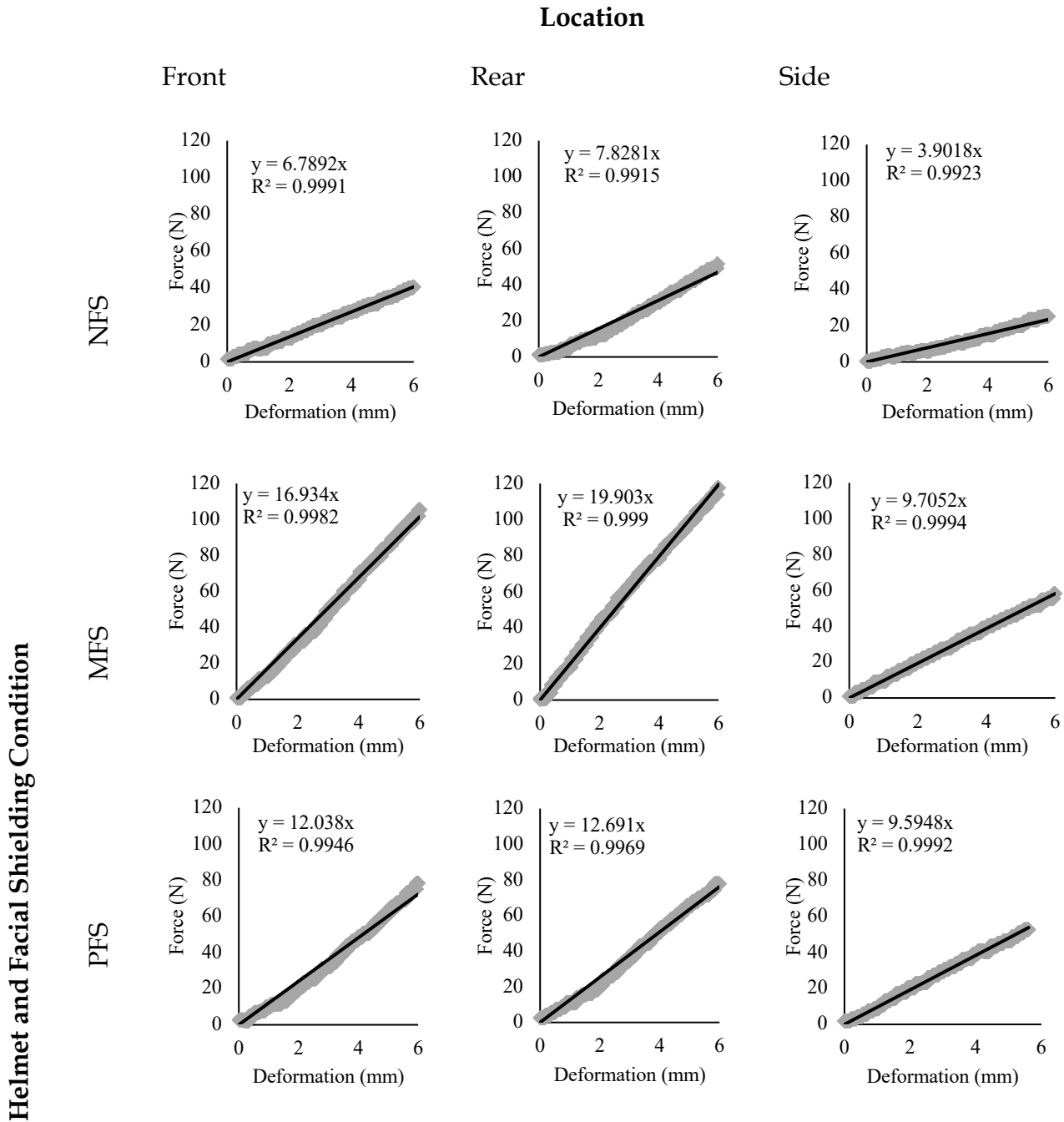


Figure 3. Stiffness of a hockey helmet with varying facial shielding conditions at the front, rear, and side locations. For each of the linear equations, y = force (N) and x = deformation (mm). The solid line indicates the interpolation line, while the shaded linear pattern illustrates the original data.

Helmet Dynamic Testing-Risk of Head Injury

A three-way mixed factorial ANOVA was conducted on GSI measures, with facial shielding and impact location as the repeated factors, and neck stiffness as the independent factor. The analysis revealed a statistically significant three-way interaction between facial shielding, impact

location, and neck stiffness on GSI measures with a large effect size indicating that the interaction explained 15% of the variance in the outcome, $F(3.28, 83.72) = 4.51, p = .004, \eta^2 = .15$. To help explain this interaction, simple two-way ANOVAs were performed with the neck stiffness levels represented by different graphs, the facial shielding conditions depicted on the horizontal axis and the helmet locations represented by different lines.

A statistically significant two-way interaction between facial shielding condition and impact location on GSI measures was observed at the low neckform stiffness level with a large effect size indicating that the interaction explained 50% of the variance in the outcome, $F(1.18, 20.12) = 17.15, p < .001, \eta^2 = .50$ (Figure 4). Simple main effect analyses were then conducted using one-way ANOVAs to determine the differences between the impact locations for each facial shielding condition on GSI measures.

The one-way ANOVA revealed a statistically significant effect of impact location on measures of GSI for helmets with NFS at the lowest neck stiffness level with a large effect size indicating that 52% of the variance in GSI can be attributed to impact location, $F(1.11, 18.84) = 18.53, p < .001, \eta^2 = .52$. A Bonferroni post-hoc analysis for pair mean comparisons revealed that the front location ($M = 536.58, SD = 444.05$) was significantly greater than the front boss ($M = 434.92, SD = 382.93$), side ($M = 313.19, SD = 292.58$), and rear ($M = 193.61, SD = 138.34$) locations for GSI measures at $p < .05$. The front boss location, on the other hand, was significantly greater than the side ($M = 313.19, SD = 292.58$) and rear ($M = 193.61, SD = 138.34$) locations for GSI measures at $p < .05$.

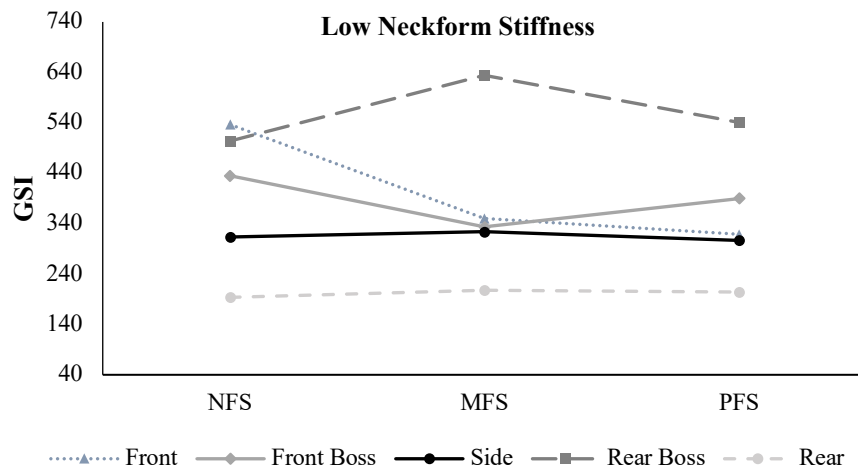


Figure 4. GSI at the low neckform stiffness level. The five impact locations (front, front boss, side, rear boss and rear) are represented by the various lines, and the facial shielding conditions on the horizontal axis are represented by the grouping labels: no facial shield (NFS), metal facial shield (MFS) and polycarbonate facial shield (PFS).

The one-way ANOVA also revealed a statistically significant effect of impact location on GSI measures for helmets with MFS at the lowest neck stiffness level with a large effect size indicating that 47% of the variance in GSI can be attributed to impact location, $F(1.03, 17.45) = 15.13, p < .001, \eta^2 = .47$. The front ($M = 350.56, SD = 286.37$), front boss ($M = 333.56, SD = 296.66$),

and side ($M = 324.00$, $SD = 284.80$) locations were significantly greater than the rear ($M = 207.73$, $SD = 150.79$) location for GSI measures at $p < .05$. The rear boss ($M = 634.11$, $SD = 611.78$) location, however, was significantly greater than the front, front boss, side, and rear location for GSI measures at $p < .05$.

Finally, the one-way ANOVA revealed a statistically significant effect of impact location for GSI measures on helmets with PFS at the lowest neck stiffness level with a large effect size indicating that 41% of the variance in GSI can be attributed to impact location, $F(1.06, 18.01) = 11.97$, $p = .002$, $\eta^2 = .41$. The front ($M = 318.78$, $SD = 233.33$) and front boss ($M = 389.92$, $SD = 350.10$) locations were significantly greater than the rear ($M = 203.84$, $SD = 145.82$) location for GSI measures at $p < .05$. In addition, the front boss location was significantly higher than the side ($M = 306.55$, $SD = 279.10$) location at $p < .05$. The rear boss ($M = 540.46$, $SD = 540.10$) location, however, it was significantly higher than the front boss, side, and rear locations at $p < .05$.

A two-way interaction between impact location and facial shielding condition was found for the GSI measures at the medium neck stiffness level with a large effect size indicating that the interaction accounted for 43% of the variance in the outcome, $F(1.36, 23.14) = 12.77$, $p < .001$, $\eta^2 = .43$ (Figure 5). Simple main effect analyses were conducted using one-way ANOVAs to determine differences between impact locations for each facial shielding condition on GSI measures.

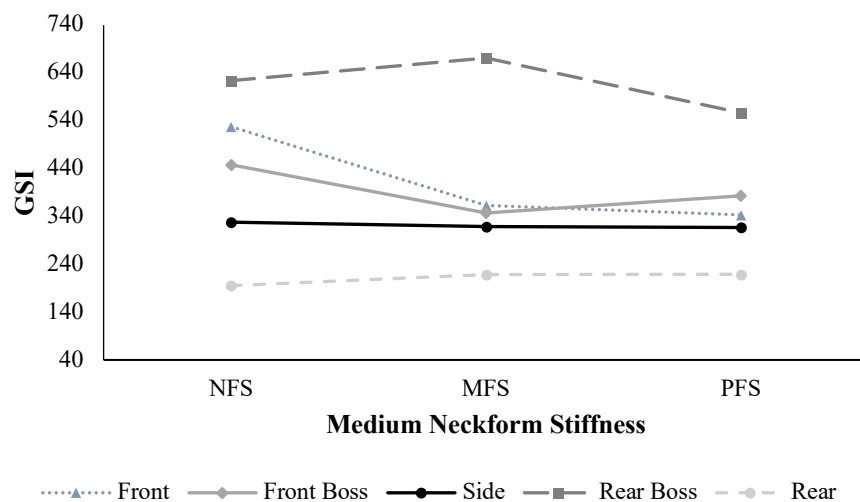


Figure 5. GSI at medium neckform stiffness. The five impact locations (front, front boss, side, rear boss and rear) are represented by the various lines, and the facial shielding conditions on the horizontal axis are represented by the grouping labels: no facial shield (NFS), metal facial shield (MFS) and polycarbonate facial shield (PFS).

The one-way ANOVA showed a significant effect of location on GSI measures for helmets NFS at the medium stiffness level with a large effect size indicating that 51% of the variance in GSI can be attributed to impact location, $F(1.03, 17.48) = 17.88$, $p < .001$, $\eta^2 = .51$. The average GSI at the front location ($M = 527.67$, $SD = 450.00$) was significantly higher than the front boss ($M = 448.07$, $SD = 409.19$), side ($M = 328.08$, $SD = 296.00$), and rear ($M = 195.30$, $SD = 149.57$) locations

at $p < .05$. Additionally, the average GSI for the front boss location was significantly greater than the side and rear locations at $p < .05$. The GSI for the side location was significantly higher than the rear location at $p < .05$. Lastly, the average GSI at the rear boss location ($M = 624.36$, $SD = 594.47$) was significantly greater than the front boss, side, and rear locations at $p < .05$.

The results of the one-way ANOVA showed a significant effect of location on GSI measures for helmets with MFS at the medium neck stiffness level with a large effect size indicating that 50% of the variance in GSI can be attributed to impact location, $F(1.04, 17.66) = 17.30$, $p < .001$, $\eta^2 = .50$. The average GSI for impacts to the front location ($M = 362.82$, $SD = 289.56$) was significantly higher than those for the side ($M = 319.57$, $SD = 281.00$) and rear ($M = 218.58$, $SD = 188.62$) locations at $p < .05$. At the meantime, the average GSI for the front boss location ($M = 347.27$, $SD = 319.30$) was significantly higher than that for the rear location, while the GSI for the side location was significantly higher than that for the rear location at $p < .05$. Furthermore, the average GSI at the rear boss location ($M = 671.28$, $SD = 634.78$) was significantly higher than that for the front, front boss, side, and rear locations at $p < .05$.

The results of the one-way ANOVA showed a significant effect of location on GSI measures for helmets with PFS at the medium neck stiffness level with a large effect size indicating that 43% of the variance in GSI can be attributed to impact location, $F(1.13, 19.21) = 12.76$, $p < .001$, $\eta^2 = .43$. Specifically, the average GSI for the front location ($M = 343.30$, $SD = 228.87$) was found to be significantly greater than the rear location ($M = 219.13$, $SD = 183.55$) at $p < .05$. The average GSI for the front boss location ($M = 383.36$, $SD = 346.93$) was significantly greater than both the side ($M = 316.93$, $SD = 285.14$) and rear ($M = 219.13$, $SD = 183.55$) locations at $p < .05$. Lastly, the average GSI at the rear boss location ($M = 556.68$, $SD = 540.52$) was significantly greater than at the front boss, side, and rear locations at $p < .05$.

A two-way interaction between impact location and facial shielding condition was also found with a large effect size indicating that the interaction accounted for 59% of the variance in the outcome, $F(1.26, 21.38) = 16.26$, $p < .001$, $\eta^2 = .59$ (Figure 6). Simple main effect analyses were conducted using one-way ANOVAs to determine differences between impact locations for each facial shielding condition.

The results of the one-way ANOVA analysis demonstrated a significant impact of location on GSI measures for helmets NFS at the highest neck stiffness level with a large effect size indicating that 53% of the variance in GSI can be attributed to impact location, $F(1.04, 17.63) = 19.20$, $p < .001$, $\eta^2 = .53$. Specifically, the GSI at the front location ($M = 578.12$, $SD = 470.99$) was found to be significantly higher than the front boss ($M = 395.41$, $SD = 343.38$), side ($M = 326.03$, $SD = 293.04$), and rear ($M = 198.68$, $SD = 153.73$) locations at $p < .05$. Additionally, the front boss location showed significantly higher GSI than the side and rear locations at $p < .05$. In turn, the side location exhibited significantly higher GSI than the rear location at $p < .05$. Finally, the average GSI at the rear boss location ($M = 663.16$, $SD = 628.88$) was significantly higher than those at the front boss, side, and rear locations at $p < .05$.

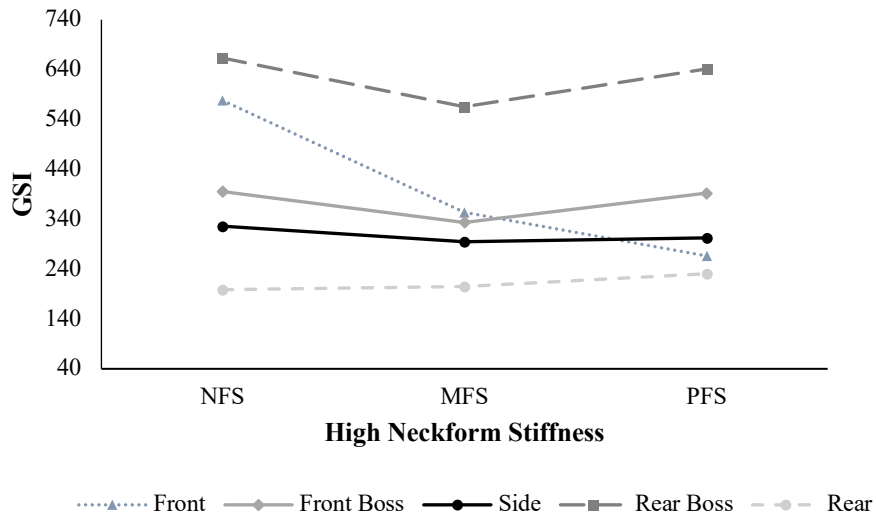


Figure 6. GSI at the high neckform stiffness. The five impact locations (front, front boss, side, rear boss and rear) are represented by the various lines, and the facial shielding conditions on the horizontal axis are represented by the grouping labels: no facial shield (NFS), metal facial shield (MFS) and polycarbonate facial shield (PFS).

The results of the one-way ANOVA indicated a significant effect of location on GSI measures for helmets with MFS at the highest stiffness level with a large effect size indicating that 42% of the variance in GSI can be attributed to impact location, $F(1.06, 17.95) = 12.29, p = .002, \eta^2 = .42$. It was found that the GSI for the front location ($M = 354.32, SD = 289.75$) was significantly higher than the side ($M = 294.79, SD = 279.45$) and rear ($M = 205.11, SD = 157.99$) locations at $p < .05$. Moreover, the GSI at the front boss location ($M = 333.40, SD = 311.14$) was significantly greater than the side and rear locations at $p < .05$. Finally, the average GSI at the rear boss location ($M = 565.50, SD = 586.43$) was significantly higher than the front boss, side, and rear locations at $p < .05$.

The results of the one-way ANOVA indicated a significant effect of location on GSI measures for helmets with PFS at the highest stiffness level with a large effect size indicating that 47% of the variance in GSI can be attributed to impact location, $F(1.06, 18.05) = 15.22, p < .001, \eta^2 = .47$. The GSI for the front boss location ($M = 392.01, SD = 350.83$) was significantly higher than the side ($M = 303.17, SD = 264.89$) and rear ($M = 230.65, SD = 204.09$) locations at $p < .05$. Additionally, the side location was significantly higher than the rear location at $p < .05$. Lastly, the average GSI at the rear boss location ($M = 641.25, SD = 605.34$) was significantly higher than the front, front boss, side, and rear locations at $p < .05$.

Across locations, 38 impacts exceeded the NOCSAE threshold GSI value of 1,200, indicating a head injury. This information is more detailed in Table 1.

Table 1. Impacts exceeding NOCSAE GSI standards.

Location	Count
Rear boss	30
Front	6
Front boss	2

Discussion

Static Stiffness Testing

The first purpose of this study was to investigate the effect of facial shielding and helmet location on measures of helmet stiffness during static testing. The researchers examined the stiffness characteristics of a hockey helmet at three different impact locations (front, rear, and side) under three facial shielding conditions (NFS, MFS, and PFS). They evaluated the helmet's stiffness based on the combined material properties of the helmet's outer shell constructed of acrylonitrile butadiene styrene (ABS) plastics, an inner liner made of VN material, an MFS manufactured from stainless steel, and a PFS composed of high impact polycarbonate material.

The average stiffness of the helmet under various facial shielding conditions at each location was determined by calculating the slope of the linear regression lines using force and deformation measures. The results revealed that the helmet outfitted with the MFS had the greatest stiffness when compared to the NFS and PFS conditions across the helmet impact locations as shown in Figure 3. This outcome corresponds with the research work of Lemair et al,³⁰ which found that the MFS had stiffer material properties than the PFS.

The results of the current study showed that adding a facial shield to the helmet diminished its ability to deform compared to helmets without the shield when subjected to the same load. As a result, the helmet became stiffer in resisting compression force, as illustrated in Figure 3. This increased stiffness may have implications during dynamic impacts. For example, the MFS, which more than doubled the stiffness of the helmet as compared to the NFS, could potentially cause permanent damage to the plastic helmet material, leading to a fracture of the helmet if it is unable to absorb impact forces.³¹ Lemair et al³⁰ observed similar outcomes, with MFS permanently deforming upon impact, while PFS deformed and then rebounded to their original shape.

The current study also found that the rear location of the helmet demonstrated the highest stiffness compared to the front and side locations, regardless of facial shielding conditions. This outcome can be attributed to the ellipsoidal nature of the human head with the long axis (the length) being greater than the short axis, the breadth.³² As a result, helmets must be designed to accommodate this shape. Geometrically, this means that the curvature at the side location of the commercial helmet used in this study is not as pronounced as it is at the front and rear locations, and consequently, the helmet seems to be less effective at distributing the load on the flatter surface. Halstead³³ also noted that the flat surfaces on hockey helmets were ineffective at spreading and deflecting the impact force and energy. Furthermore, in the current study, when loaded at the front and rear sites, the aperture of the helmet became more circular, whereas

when compressed at the side, the helmet became more ellipsoidal. Putting together these pieces of evidence, the ellipsoidal geometry of the helmet helps explain why the front and rear locations exhibited similar stiffness properties. This information is very useful in helmet design and testing to better understand the capabilities of the helmet material to withstand and mitigate impact forces before being exposed to dynamic collision at different helmet locations. It is conceivable, however, that the anticipated performance of a helmet based on the static results may be altered during dynamic impact as a result of other factors, including the stiffness of athletes' necks and the geometrical structure of the helmet to overcome specific mechanisms of the impact.

Dynamic Impact Testing

Simulating helmet impacts in a laboratory setting is crucial for understanding the injury mechanisms experienced by athletes in a game and the capabilities of helmet material to mitigate forces during dynamic collisions. In Canada, over 475,000 hockey players, approximately 75% of the total, are required to wear full facial shielding.³⁴ Consequently, most players who experienced head contact would very likely be wearing a helmet with full facial protection. It is, therefore, critical to understand the extent to which a helmet's facial shielding minimizes head injuries upon impact.

One approach to assess the severity of head injury is by simulating the injury mechanism and estimating the GSI values for any given impact on the helmet taking into consideration the level of neck strength and the type of facial shielding condition. The current study used this approach, and the results indicated a significant combined effect of facial shielding condition and impact location on GSI measures across different levels of neck stiffness. These findings are crucial, as impact location is associated with the player's susceptibility to concussions.⁶

In the current study, helmets with NFS and MFS displayed significant main effects of impact location at each level of neck stiffness on GSI measures. The rear boss location produced the greatest risk of injury value, followed by the front, front boss, side, and rear locations as shown in Figures 4 and 5. Helmets with PFS also exhibited significant main effects at each neck stiffness level. For PFS, the rear boss location had the highest GSI value, while the rear location had the lowest, with other impact locations (front boss, side, and front) showing no consistent trends across neck stiffness levels.

The helmets were visually inspected to identify possible reasons for the varying GSI values at the different impact locations of the helmets. It was observed that the rear boss location had less attenuation lining on the area of impact, which meant that the force was not sufficiently dissipated and was instead transferred to the headform. In contrast, the rear location had the lowest GSI values, which corresponded to having the thickest lining. Furthermore, it was noticed that the MFS had the highest GSI values at the rear boss location compared to the other face shields as shown in Figures 4 and 5. This outcome can be attributed to the increased stiffness of the helmet due to fitting it with a MFS, which had the highest stiffness as shown in Figure 3. When the stiffness of the MFS combined with the reduced amount of attenuation lining at the

rear boss location, it led to higher linear impact accelerations and, consequently, increased GSI values compared to the NFS and PFS, which were less stiff.

These findings confirm that helmet performance in reducing impact severity is non-uniform across impact locations during dynamic collision and the outcome may not be as expected from the static measures. For example, the rear location of the helmet displayed the highest stiffness but was associated with the lowest risk of injury value. To further support this outcome, 38 instances in this study exceeded the NOCSAE threshold GSI value of 1,200, indicating a head injury. Thirty of these impacts occurred at the rear boss, six at the front, and two at the front boss locations. The geometry of the helmet, with and without facial shielding, likely contributed to these high GSI values due to the increased linear impact acceleration.¹⁶

These results, however, align with the research by Caswell et al³⁵ which found differences in impact severity between front and rear boss locations on lacrosse helmets. It is interesting to note that lacrosse helmets are usually worn with a face shield. Similarly, Carlson¹⁴ reported a significant main effect of impact location on GSI. However, there are key differences between the current study and Carlson's research. These differences include the type of helmet brand and model, helmet geometry, and the position of attenuation liners, which influence GSI measures.¹⁶ Furthermore, the current study simulated horizontal collisions using a pneumatic system, whereas Carlson's study simulated vertical free falls using a drop testing system.¹⁴ Additionally, Carlson's study did not consider facial shielding, focusing instead on impact angle.¹⁴ Despite these differences, both studies indicated that an athlete's risk of injury depends on the helmet's impact location. The current study extends Carlson's findings by suggesting that injury risk also depends on the type of facial shielding attached to the actual helmet.

Interestingly, the side impact location did not yield the highest GSI values, a promising outcome since lateral impacts are often associated with a higher concussion risk.¹² As noted, the rear boss location had the greatest injury likelihood, followed by the front and front boss locations for NFS and MFS, and by the front boss and side locations for PFS, respectively. These results are consistent with Carlson's¹⁴ and support those of Caswell et al³⁵ regarding lacrosse helmets. Caswell et al³⁵ found that NFS helmets typically had the highest GSI measures, exceeding the critical value of 1,200 in 17 instances. Helmets with MFS followed, with 11 instances exceeding the threshold. PFS had the lowest GSI measures and the fewest instances, with 10 exceeding the threshold. Lemair et al³⁰ reported similar trends when directly impacting different facial shields. A combination of the material properties of both MFS and PFS may help minimize GSI and enhance the protective capabilities of the helmet during dynamic impacts.

The higher GSI measures for NFS helmets, however, can be attributed to the added mass of the shielding, increasing system inertia and resulting in lower acceleration values.³² This study supports this rationale, showing lower GSI values for helmets with facial shields. However, it may also be possible that adding the extra mass can increase the GSI, especially for individuals with lower neck strength levels as shown in Figures 4 and 5. Furthermore, it is important to note that the NFS condition did not always produce the highest GSI measures across different neck stiffness levels. Nonetheless, this study is the first to test both PFS and MFS on hockey helmets across various impact locations and neck stiffness levels concerning GSI measures.

To summarize, the primary strength of this study was the comparative analysis of helmets with two types of facial shields against helmets without facial shields, utilizing a horizontal impactor to simulate on-ice collisions. Unlike Lemair et al.³¹ who directly impacted the facial shields using a drop testing method, this study focused on five NOCSAE impact locations on helmets without directly impacting the facial shields. The headform, instrumented with accelerometers, measured linear accelerations due to impact; however, it did not measure rotational acceleration, a critical variable associated with concussions and brain injuries.³⁶ It is also possible that the helmet deteriorates over repetitive impacts diminishing its capability to mitigate impact acceleration. In the current study, however, a durability test was conducted based on the work of Carlson¹⁴ and it was deemed appropriate that a helmet could receive 54 impacts in one location before being replaced to maintain the integrity of the data. Despite this limitation, this study effectively examined the influence of neck stiffness levels, helmet impact locations, and facial shielding conditions on injury risk using impact acceleration measures to estimate GSI based on the NOCSAE helmet testing protocol.

This study examined the effect of facial shielding and helmet location on measures of helmet stiffness during static testing. The study also examined the effects of impact location, facial shielding condition, and neck stiffness on GSI measures. The static results provided a better understanding of the capabilities of the helmet material to withstand and mitigate impact forces before being exposed to dynamic collision at different helmet locations. The dynamic results build on Lemair et al.³⁰ by providing new insights into how facial shielding affects GSI measures when the shield is not directly impacted but is present on the helmet. The findings offer a more comprehensive understanding of how helmet and facial shielding combinations affect a player's vulnerability to injury. Further investigation into helmet material properties across locations, however, is needed to better understand the risk of head injury and concussions when wearing protective devices.^{14, 18, 30}

Future research should continue to explore the relationship between facial shielding and helmet performance in reducing impact severity. Such research could assist manufacturers in improving the design of facial shields and their attachment mechanisms as shown in Figures 1 and 2 to better protect players from the impacts encountered in hockey.³⁷ Testing organizations may consider incorporating facial shielding in their impact assessments, as full facial protection is prevalent among players.

References

1. Agel J, Harvey EJ. A 7-year review of men's and women's ice hockey injuries in the NCAA. *Can J Surg.* 2010;53(5):319-323. <https://pubmed.ncbi.nlm.nih.gov/20858376/>
2. Biasca N, Wirth S, Maxwell W, Simmen H-P. Minor traumatic brain injury (mTBI) in ice hockey and other contact sports. *Eur J Trauma.* 2005;31(2):105-116. <https://doi.org/10.1007/s00068-005-1050-z>
3. Mayo Clinic. Concussion. Accessed February 18, 2025. <https://www.mayoclinic.org/diseases-conditions/concussion/symptoms-causes/syc-20355594>
4. Giza CC, Hovda DA. The neurometabolic cascade of concussion. *J Athl Train.* 2001;36(3):228-235. <https://pmc.ncbi.nlm.nih.gov/articles/PMC155411/>

5. Andrews E, Jildeh TR, Abbas MJ, Lindsay-Rivera K, Berguson J, Okoroha KR. Concussion in the National Hockey League: Analysis of Incidence, Return to Play, and Performance. *Orthop J Sports Med.* 2022;10(1):1-6. <https://doi.org/10.1177/23259671211052069>
6. Greenwald RM, Gwin JT, Chu JJ, Crisco JJ. Head impact severity measurement for evaluating mild traumatic brain injury risk exposure. *Neurosurg.* 2008;62(4):789-798. <https://doi.org/10.1227/01.neu.0000318162.67472.ad>
7. Rybak T, Sanzo P, Liu M, Zerpa C. Evaluating the effectiveness of boxing headguards in mitigating head impact acceleration that causes concussions using a dynamic head model. *Int J Extreme Autom Connect Health Care.* 2023;5(1):1-15. <https://doi.org/10.4018/ijeach.319811>
8. Zhang L, Yang KH, King AI. A proposed injury threshold for mild traumatic brain injury. *J Biomech Eng.* 2004;126(2):226-236. <https://doi.org/10.1115/1.1691446>
9. Gurdjian ES. Recent advances in the study of the mechanism of impact injury the head-a summary. *Clin Neurosurg.* 1972;19:1-42. https://doi.org/10.1093/neurosurgery/19.CN_suppl_1.1
10. Ouckama R. *Time series measurement of force distribution in ice hockey helmets during varying impact conditions.* Dissertation. McGill University; 2013. Accessed February 18, 2025. <https://escholarship.mcgill.ca/concern/theses/6969z4213>
11. Zhang L, Yang KH, King AI. Comparison of brain responses between frontal and lateral impacts by finite element modelling. *J Neurotrauma.* 2011;18(1):21-30. <https://doi.org/10.1089/08977150175005574>
12. Hodgson VR, Thomas LM, Khalil TB. The role of impact location in reversible cerebral concussion. In: *Proceedings of the 27th Stapp Car Crash Conference.* Stapp Association; 1983; SAE Paper No. 831618. <https://doi.org/10.4271/831618>
13. Walsh ES, Rousseau P, Hoshizaki TB. The influence of impact location and angle on the dynamic impact response of a Hybrid III headform. *Sports Eng.* 2011;13(3):135-143. <https://doi.org/10.1007/s12283-011-0060-9>
14. Carlson S. *The influence of neck stiffness, impact location, and angle on peak linear acceleration, shear force, and energy loading measures of hockey helmet impacts.* Master's thesis. Lakehead University; 2016. Accessed February 18, 2025. [The Influence of Neck Stiffness, Impact Location, and Angle on Peak Linear Acceleration, Shear Force, and Energy Loading Measures of Hockey Helmet Impacts](https://doi.org/10.1007/s12283-011-0060-9)
15. Pennock B, Kivi D, Zerpa C. Effect of neck strength on simulated head impacts during falls in females ice hockey players. *Int J Exerc Sci.* 2021;14(1):446-461. <https://doi.org/10.70252/OXUE1359>
16. Rousseau P, Hoshizaki TB. The influence of deflection and neck compliance on the impact dynamics of a Hybrid III headform. *Proceedings of the Institution of Mechanical Engineers, Part P: Journal of Sports Engineering and Technology.* 2009;223(3):89-97. <https://doi.org/10.1243/17543371JSET34>
17. Rowson S, Bland ML, Campolettano ET, Press JN, Rowson B, Smith JA, Sproule DW, Tyson AM, Duma SM. Biomechanical perspectives on concussion in sport. *Sports Med Arthrosc Rev.* 2016;24(3):100-107. <https://doi.org/10.1097/JSA.0000000000000121>
18. Kaplan S, Driscoll CF, Singer MT. Fabrication of a facial shield to prevent facial injuries during sporting events: a clinical report. *J Prosthet Dent.* 2000;84(4):387-389. <https://doi.org/10.1067/mpr.2000.109480>
19. Rowson S, Duma SM. Development of the STAR evaluation system for football helmets: Integrating player head impact exposure and risk of concussion. *Ann Biomed Eng.* 2011;39(8):2130-2140. <https://doi.org/10.1007/s10439-011-0322-5>
20. Hall SJ. *Basic Biomechanics.* 6th ed. McGraw-Hill; 2007.

21. National Operating Committee on Standards for Athletic Equipment. Standard test method and equipment used in evaluating the performance characteristics of headgear/equipment (ND 001-15m15b). 2017. Accessed February 18, 2025. <https://nocsae.org/nd001-historical-versions/>
22. Halstead ME, Walter KD, Moffatt K, Council on Sports Medicine and Fitness. Sport-related concussion in children and adolescents. *Pediatrics*. 2010;126(3):597-615. <https://doi.org/10.1542/peds.2018-3074>
23. Graham R, Rivara FP, Ford, MA, Spicer CM. *Sports-related concussions in youth*. The National Academies Press; 2014.
24. Asplund C, Bettcher S, Borchers J. Facial protection and head injuries in ice hockey: a systematic review. *Br J Sports Med*. 2009;43(13):993-999. <https://doi.org/10.1136/bjsm.2009.060152>
25. Stuart MJ, Smith AM, Malo-Ortiguera SA, Fischer TL, Larson DR. A comparison of facial protection and the incidence of head, neck, and facial injuries in Junior A hockey players: A function of individual playing time. *Am J Sports Med*. 2002;30(1):39-44. <https://doi.org/10.1177/03635465020300012001>
26. Benson BW, Hamilton GM, Meeuwisse WH, McCrory P, Dvorak J. Is protective equipment useful in preventing concussion? A systematic review of the literature. *Br J Sports Med*. 2009;43(1):56-67. <https://doi.org/10.1136/bjsm.2009.058271>
27. Baumgart F. Stiffness – an unknown world of mechanical science? *Injury*. 2000;31(2):14-23, 72, 76, 80, 84. [https://doi.org/10.1016/S0020-1383\(00\)80040-6](https://doi.org/10.1016/S0020-1383(00)80040-6)
28. Navalta JW, Stone WJ, Lyons TS. Ethical issues relating to scientific discovery in exercise science. *Int J Exerc Sci*. 2019;12(1):1-8. <https://doi.org/10.70252/EYCD6235>
29. Zerpa C, Carlson S, Przyucha E, Liu M, Sanzo P. Evaluating the performance of a hockey helmet in mitigating concussion risk using measures of acceleration and energy during simulated free fall. *Int J Extreme Autom Connect Health Care*. 2021;3(2):33-50. <https://doi.org/10.4018/IJEACH.2021070104>
30. Lemair M, Pearsall DJ. Evaluation of impact attenuation of facial protectors in ice hockey helmets. *Sports Eng*. 2007;10(2):65-74. <https://doi.org/10.1007/BF02844204>
31. Craig R, Kurdila A. *Mechanics of Materials*. John Wiley & Sons; 1996.
32. Young JW, Federal Aviation Administration. Head and face anthropometry of adult US civilians (Final Report). 1993. Accessed February 18, 2025. https://www.faa.gov/sites/faa.gov/files/data_research/research/med_humanfacs/oamtechreports/AM93-10.pdf
33. Halstead PD, Alexander CF, Cook EM, Drew RC. Hockey headgear and the adequacy of current designs and standards. In: Ashare AB, ed. *Safety in Ice Hockey: Third Volume*. ASTM International; 2000;93-100. <https://doi.org/10.1520/STP15230S>
34. Hockey Canada. 2015-16 Annual report. 2015. Accessed February 18, 2025. [2015-16 annual report e.pdf](#)
35. Caswell SV, Deivert RG. Lacrosse helmet designs and the effects of impact forces. *J Athl Train*. 2002;37(2):164-171. <https://pubmed.ncbi.nlm.nih.gov/12937430/>
36. Hoshizaki T, Post A, Zerpa C, Legace E, Hoshizaki, T. Blaine, Gilchrist, M. Evaluation of tow rotational helmet technologies to decrease rotational acceleration in cycling helmets. *Sci Rep*. 2022;12(1):7735. <https://doi.org/10.1038/s41598-022-11559-0>

37. Canadian Standards Association. Face protectors for use in ice hockey (Z262.2-15 R2019). 2015. Accessed February 18, 2025. [Z262.2-15 \(R2019\) | Product | CSA Group](#)

